

Structural, spectroscopic and angular-overlap studies of tripodal pyridine ligands with nickel(II) and zinc(II)

Timothy Astley,*†^a Michael A. Hitchman,^a F. Richard Keene^b and Edward R. T. Tiekink^c

^a Chemistry Department, University of Tasmania, Hobart, Tasmania 7001, Australia

^b Department of Molecular Sciences, James Cook University of North Queensland, Townsville, Queensland 4811, Australia

^c Department of Chemistry, The University of Adelaide, Adelaide, South Australia 5005, Australia

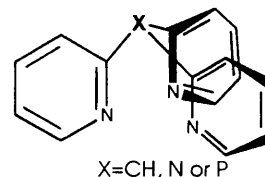
Zinc(II) and nickel(II) complexes $[M\{X(C_5H_4N)_3\}_2]^{2+}$, where $X(C_5H_4N)_3$ are symmetrical tripodal nitrogen-donor ligands with $X = CH, N$ or P , have been prepared and examined by single-crystal X-ray diffraction and single-crystal electronic spectroscopy. The structural studies, and the application of the angular overlap model to the spectroscopic results, confirm previous results on the bonding characteristics of pyridine and provide a unique way of establishing the effect of the bridgehead atom, X . The cations are all centrosymmetric with the ligand 'bite' angles $N-M-N$ $85.2(1)$ – $88.5(2)^\circ$, resulting in a slight trigonal distortion from octahedral geometry. The ligand fields in the three nickel compounds are very similar and the large ligand-field splitting is consistent with the rather short metal–nitrogen bond lengths. The pyridine groups act as moderately strong σ -donor and weak π -donor ligands, with no evidence of conjugation of the π system across the bridgehead atom. The crystal structure of $[Ni\{CH(C_5H_4N)_3\}_2][NO_3]_2$ shows the complex cation to have crystallographic $\bar{3}$ symmetry such that there is one independent Ni–N interaction of $2.069(2)$ Å. The corresponding zinc complex, isolated as its dibromide nonahydrate salt, has crystallographic $2/m$ symmetry with two Zn–N contacts of $2.123(5)$ Å being shorter than the others, *i.e.* $2.141(3)$ Å. In the phosphine analogue, $[Zn\{P(C_5H_4N)_3\}_2]^{2+}$, isolated as its diperchlorate monohydrate salt, the Zn^{2+} cation is situated on a site of symmetry $\bar{1}$ with one Zn–N distance [$2.145(4)$ Å] being shorter than the other two, $2.162(4)$ and $2.173(4)$ Å. Small trigonal distortions from the ideal octahedral geometry are due to the restricted bite distances of the tripodal ligands.

Recent work from our laboratories has concentrated on furthering understanding of the bonding properties of polydentate ligands containing heterocycles, especially pyridine and pyrazole.^{1,2} For ligands of the type $(pz)_3CH$, where $pz =$ pyrazol-1-yl, it was found² that there is no evidence of conjugation between the heterocyclic rings. The high ligand-field strength of $(pz)_3CH$ was explained using the angular overlap model (AOM) as arising from the short metal–ligand bonds imposed by the tripodal nature of the ligand. As part of this study the compounds, tris(2-pyridyl)-methane, -phosphine and -amine have been synthesized. The complexes formed by $(NC_5H_4)_3CH$ enable a comparison of the bonding characteristics of pyrazole and pyridine. In addition, the analogous complexes formed by compounds in which the bridgehead atom is altered to P or N indicate the effect on the stereochemistry and bonding properties of an alteration of this feature.

Experimental

Tris(2-pyridyl)-methane, -phosphine and -amine were prepared using published methods.³ The purity of the complexes was checked by microanalysis performed by the Central Science Laboratory, Hobart, Tasmania and Chemical and Micro Analytical Services Pty. Ltd., Melbourne, Victoria. Single-crystal and KBr disc electronic spectra were recorded using either a Cary 17 or 5 spectrophotometer as described in detail elsewhere,⁴ with the samples cooled using a Cryodyne model 22C cryostat. Absorption coefficients were estimated by measuring the crystal thickness using a microscope with a graduated eyepiece. Reflectance spectra were recorded using a Beckmann DK-2A ratio recording spectrophotometer.

† Present address: Chemistry Department, University of Reading, Whiteknights Park, Reading RG6 2AD, UK.



Synthesis of metal(II) complexes

Bis[tris(2-pyridyl)methane]nickel(II) nitrate, $[Ni\{CH(C_5H_4N)_3\}_2][NO_3]_2 \cdot 6H_2O$. A solution of $Ni(NO_3)_2 \cdot 6H_2O$ (145 mg, 0.5 mmol) in acetone (5 cm³) was added dropwise to a stirred solution of tris(2-pyridyl)methane (250 mg, 1 mmol) in acetone (10 cm³). The resulting suspension was cooled at 0 °C for 2 h, filtered, washed with acetone and air dried. Yield: 260 mg, 77%. Crystals were grown by liquid diffusion of a solution of the complex in acetonitrile layered on top of toluene (Found: C, 56.7; H, 3.95; N, 16.4. Calc. for $C_{32}H_{26}N_8NiO_6$: C, 56.7; H, 3.85; N, 16.5%).

Bis[tris(2-pyridyl)phosphine]nickel(II) nitrate, $[Ni\{P(C_5H_4N)_3\}_2][NO_3]_2 \cdot H_2O$ and **bis[tris(2-pyridyl)amine]nickel(II) perchlorate**, $[Ni\{N(C_5H_4N)_3\}_2][ClO_4]_2 \cdot 2H_2O$. The nitrate salts were prepared in an analogous manner to that the $(NC_5H_4)_3CH$ complex (yields 73% and 70%, respectively) and the latter species was converted into the perchlorate salt by metathesis in aqueous solution (Found: C, 48.8; H, 3.15; N, 14.6. Calc. for $C_{30}H_{26}N_8NiO_7P_2$: C, 49.2; H, 3.60; N, 15.3. Found: C, 47.5; H, 3.20; N, 14.7. Calc. for $C_{30}H_{24}Cl_2N_8NiO_8$: C, 47.8; H, 3.20; N, 14.9%).

Bis[tris(2-pyridyl)methane]zinc(II) nitrate, $[Zn\{CH(C_5H_4N)_3\}_2][NO_3]_2$. A solution of $Zn(NO_3)_2 \cdot 6H_2O$ (150 mg, 0.5

mmol) in acetone (5 cm³) was added dropwise to a stirred solution of tris(2-pyridyl)methane (250 mg, 1 mmol) in acetone (10 cm³). The resulting suspension was cooled at 0 °C for 2 h, filtered, washed with acetone and air dried. Yield: 320 mg, 94%. A sample of the nitrate salt was converted into the bromide using anion-exchange chromatography, and crystals of [Zn{CH(C₅H₄N)₃}₂]Br₂·9H₂O were grown by slow evaporation of an aqueous solution (Found: C, 43.2; H, 4.45; N, 9.2. Calc. for C₃₂H₄₄Br₂N₆O₉Zn: C, 43.6; H, 5.05; N, 9.5%).

The complex [Zn{P(C₅H₄N)₃}₂][NO₃]₂ was prepared in an analogous manner (yield: 340 mg, 95%). A sample of the nitrate salt was converted into the perchlorate by metathesis in aqueous solution, and crystals of [Zn{P(C₅H₄N)₃}₂][ClO₄]₂·H₂O were grown by slow evaporation of an aqueous solution (Found: C, 45.5; H, 3.00; N, 10.3. Calc. for C₃₀H₂₄Cl₂N₆O₈P₂Zn: C, 45.3; H, 3.05; N, 10.6%).

Crystallography

Intensity data for a mauve crystal of [Ni{CH(C₅H₄N)₃}₂][NO₃]₂ (0.13 × 0.29 × 0.29 mm) and colourless crystals of [Zn{CH(C₅H₄N)₃}₂]Br₂·9H₂O (0.13 × 0.24 × 0.40 mm) and [Zn{P(C₅H₄N)₃}₂][ClO₄]₂·H₂O (0.16 × 0.16 × 0.32 mm) were measured at 293 K on a Rigaku AFC6R diffractometer fitted with graphite-monochromatized Mo-Kα radiation, λ = 0.710 73 Å; the ω–2θ scan technique was employed to measure data such that θ_{max} was 27.5°. No decomposition of the crystals occurred during their respective data collections and only absorption-corrected data⁵ which satisfied the criterion $I \geq 3.0\sigma(I)$ were used in the subsequent analyses. Crystal data are summarized in Table 5.

Each structure was solved by heavy-atom methods and the remaining atoms located from subsequent difference maps; the structures were refined by a full-matrix least squares based on F_o^2 ,⁶ such that the function minimized was $\sum w\Delta^2$ where w was the weight applied to each reflection and $\Delta = |F_o| - |F_c|$. Non-hydrogen atoms were refined with anisotropic thermal parameters, the only exception being for the isotropic refinement of the O(4) atom in [Zn{CH(C₅H₄N)₃}₂]Br₂·9H₂O; this atom was found to be disordered over the two-fold axis and was refined with 0.5:0.5 site occupancy. The H atoms were located from difference maps for the (NC₅H₄)₃CH complexes and included in the models but not refined. In the case of the P(C₅H₄N)₃ complex the H atoms were included at their calculated positions (C–H 0.97 Å); water-bound hydrogen atoms were not located in the zinc complexes. At convergence $R = 0.043$ and $R' = 0.047$ (unit weights) for [Ni{CH(C₅H₄N)₃}₂][NO₃]₂, 0.041 and 0.051 [sigma weights, *i.e.* $1/\sigma^2(F)$] for [Zn{CH(C₅H₄N)₃}₂]Br₂·9H₂O and 0.049 and 0.049 (unit weights) for [Zn{P(C₅H₄N)₃}₂][ClO₄]₂·H₂O. No corrections were applied for extinction effects. Scattering factors for all atoms were those incorporated in the TEXSAN program. Fractional atomic coordinates are listed in Tables 6–8; structures were drawn with the ORTEP program.⁷

Complete atomic coordinates, thermal parameters and bond lengths and angles have been deposited at the Cambridge Crystallographic Data Centre. See Instructions for Authors, *J. Chem. Soc., Dalton Trans.*, 1996, Issue 1.

Results and Discussion

Crystal Structures of the complexes

The compounds are all quite different. Whilst they contain a basically similar cation [ML₂]²⁺ each involves a different

* The freshly isolated crystal used in the crystal structure was the monohydrate: on a slightly longer time-scale it is clear that loss of the water of crystallization occurs from the sample, as it was analysed as the anhydrous salt.

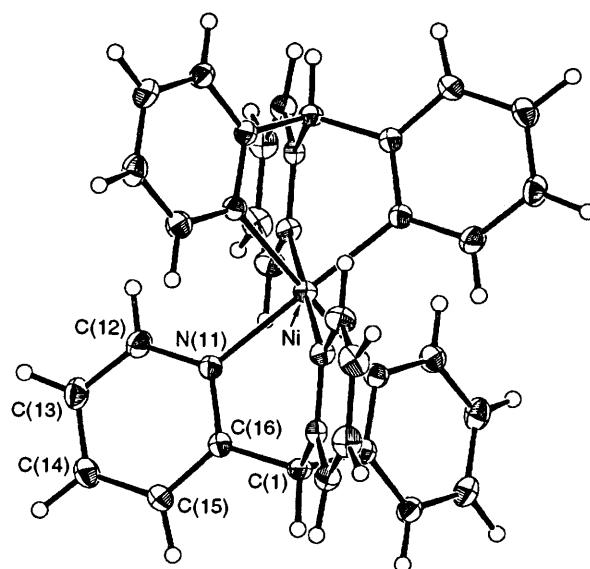


Fig. 1 Molecular structure and crystallographic numbering scheme for the cation in [Ni{CH(C₅H₄N)₃}₂][NO₃]₂

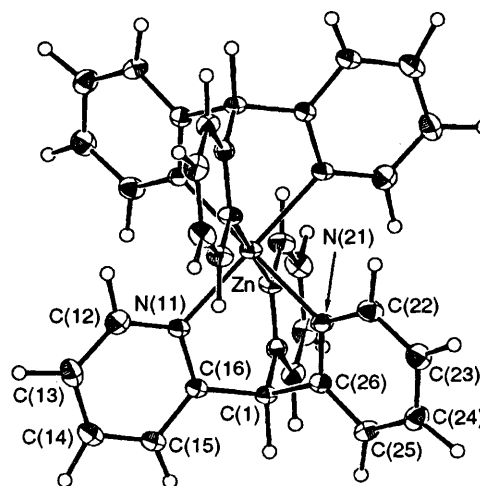


Fig. 2 Molecular structure and crystallographic numbering scheme for the cation in [Zn{CH(C₅H₄N)₃}₂]Br₂·9H₂O

anion and has a varying degree of solvation, with the nickel(II) complex being unsolvated and the [Zn{CH(C₅H₄N)₃}₂]Br₂ compound having nine waters of solvation. In each case the metal lies on a crystallographic inversion centre. All structures are essentially ordered, without the disorder found in [Cu{CH(C₅H₄N)₃}₂]²⁺⁸ and the complexes formed by bis(pyrazol-1-yl)(2-pyridyl)methane.¹

The metal–pyridine bond lengths are significantly shorter than those in complexes involving monodentate pyridine ligands, 2.069(2) Å in the nickel compound for instance, compared with 2.14 Å.⁹ However, they are comparable to those in [M{CH(C₅H₄N)(pz)₂}₂][NO₃]₂, where the Ni–N bond length is 2.076(5) Å.¹ For all of the complexes the ‘bite’ of the tripodal ligand and the ligand geometry results in an unsymmetrical orientation of each ring with respect to the M–N direction. In the (NC₅H₄)₃CH complexes the M–N–C(6) angles are between 117.5(2) and 118.3(4)° and the M–N–C(2) angles are significantly larger, being between 123.2(3) and 128.8(2)°. This effect is not seen for the P(C₅H₄N)₃ complex [M–N–C(6) 120.4(3)–122.5(4), M–N–C(2) 120.5(4)–121.5(4)°] presumably because the larger size of the bridgehead atom allows the pyridine rings to orientate more directly along the M–N axis.

The average Zn–N bond lengths are considerably longer than those involving Ni, as expected from the ionic radii of the divalent metal ions. The planes of the amine rings make angles

Table 1 Selected bond distances (Å) and angles (°) for $[\text{Ni}\{\text{CH}(\text{C}_5\text{H}_4\text{N})_3\}_2][\text{NO}_3]_2$

Ni–N(11)	2.069(2)	N(11)–C(12)	1.339(4)
N(11)–C(16)	1.335(4)	C(1)–C(16)	1.497(3)
C(12)–C(13)	1.348(5)	C(13)–C(14)	1.375(5)
C(14)–C(15)	1.370(5)	C(15)–C(16)	1.369(4)
N(1)–O(1)	1.235(3)		
N(11)–Ni–N(11 ¹)	93.5(1)	Ni–N(11)–C(12)	123.8(2)
Ni–N(11)–C(16)	118.7(2)	C(12)–N(11)–C(16)	117.5(3)
C(16)–C(1)–C(16 ^h)	111.3(2)	N(11)–C(12)–C(13)	123.5(3)
C(12)–C(13)–C(14)	118.9(3)	C(13)–C(14)–C(15)	118.6(3)
C(14)–C(15)–C(16)	119.4(3)	N(11)–C(16)–C(15)	122.1(3)
N(11)–C(16)–C(1)	116.6(3)	C(1)–C(16)–C(15)	121.2(3)

Symmetry operations: I $x - y, -1 + x, 2 - z$, II $1 - y, -1 + x - y, z$.

Table 2 Selected bond distances (Å) and angles (°) for $[\text{Zn}\{\text{CH}(\text{C}_5\text{H}_4\text{N})_3\}_2]\text{Br}_2 \cdot 9\text{H}_2\text{O}$

Zn–N(11)	2.123(5)	Zn–N(21)	2.141(3)
N(11)–C(12)	1.320(8)	N(11)–C(16)	1.335(7)
N(21)–C(22)	1.320(5)	N(21)–C(26)	1.329(5)
C(1)–C(16)	1.505(8)	C(1)–C(26)	1.513(5)
C(12)–C(13)	1.366(9)	C(13)–C(14)	1.367(9)
C(14)–C(15)	1.357(9)	C(15)–C(16)	1.361(8)
C(22)–C(23)	1.358(6)	C(23)–C(24)	1.369(6)
C(24)–C(25)	1.364(6)	C(25)–C(26)	1.360(6)
N(11)–Zn–N(21)	85.3(1)	N(21)–Zn–N(21 ¹)	86.1(2)
Zn–N(11)–C(12)	123.5(4)	Zn–N(11)–C(16)	118.3(4)
Zn–N(21)–C(22)	123.4(3)	Zn–N(21)–C(26)	118.1(3)
C(12)–N(11)–C(16)	118.2(5)	C(22)–N(21)–C(26)	118.4(4)
C(16)–C(1)–C(26)	111.8(3)	C(26)–C(1)–C(26 ¹)	110.5(5)
N(11)–C(12)–C(13)	123.2(6)	C(12)–C(13)–C(14)	117.8(6)
C(13)–C(14)–C(15)	119.6(6)	C(14)–C(15)–C(16)	119.4(6)
N(11)–C(16)–C(1)	117.7(5)	N(11)–C(16)–C(15)	121.7(5)
C(1)–C(16)–C(15)	120.5(5)	N(21)–C(22)–C(23)	123.3(4)
C(22)–C(23)–C(24)	117.9(4)	C(23)–C(24)–C(25)	119.3(4)
C(24)–C(25)–C(26)	119.3(4)	N(21)–C(26)–C(1)	117.6(4)
N(21)–C(26)–C(25)	121.7(4)	C(1)–C(26)–C(25)	120.6(4)

Symmetry operation: I $x, -y, z$.

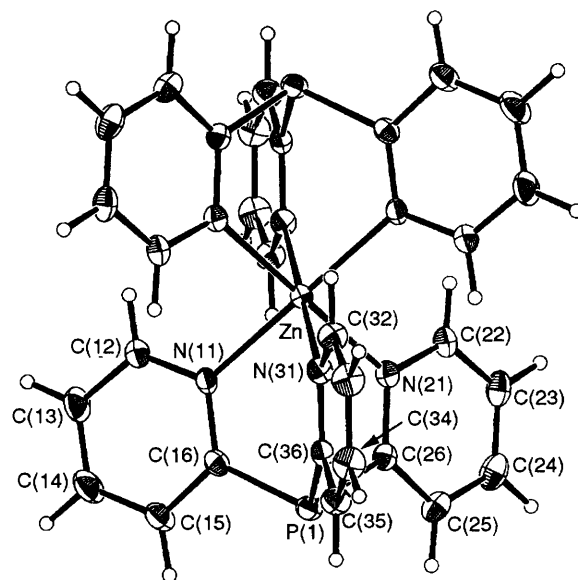
of $\approx 40^\circ$ with those defined by the M–N bond vectors, resulting in a ‘paddlewheel’ conformation about the trigonal axis as found in the $(\text{NC}_5\text{H}_4)_3\text{CH}$ complexes.²

$[\text{Ni}\{\text{CH}(\text{C}_5\text{H}_4\text{N})_3\}_2][\text{NO}_3]_2$. The structure of the cation is shown in Fig. 1 and selected interatomic parameters are listed in Table 1. The structure comprises discrete entities with the closest non-H interionic contact occurring between the O(1) and C(13) atoms of 3.290(5) Å. The structure is isomorphous with the copper(II) analogue⁸ and the Ni^{2+} is situated on a crystallographic site of symmetry $\bar{3}$. The six Ni–N bonds are equivalent at 2.069(2) Å. The major distortion from the ideal octahedral geometry is found in the chelate angles of 86.5(1)° which arise as a result of the restricted bite angles of the $(\text{NC}_5\text{H}_4)_3\text{CH}$ ligand.

$[\text{Zn}\{\text{CH}(\text{C}_5\text{H}_4\text{N})_3\}_2]\text{Br}_2 \cdot 9\text{H}_2\text{O}$. The structure of the cation is shown in Fig. 2 and selected interatomic parameters are listed in Table 2. The structure crystallizes in the monoclinic space group $C2/m$ with two complex cations, four bromides and eighteen water molecules of crystallization comprising the unit-cell contents. The Zn^{2+} cation is located on a site of symmetry $2/m$, the methine C(1) atom and pyridine ring N(11)–C(16) on a mirror plane, and the N(21)–C(26) ring in a general position. In the lattice there is, as expected, a complicated network of intermolecular contacts involving ions and water molecules. The Br atom forms four contacts with water molecules in the range 3.363(4)–3.480(5) Å and the closest contact involving

Table 3 Selected bond distances (Å) and angles (°) for $[\text{Zn}\{\text{P}(\text{C}_5\text{H}_4\text{N})_3\}_2][\text{ClO}_4]_2 \cdot \text{H}_2\text{O}$

Zn–N(11)	2.162(4)	Zn–N(21)	2.145(4)
Zn–N(31)	2.173(4)	P(1)–C(16)	1.816(6)
P(1)–C(26)	1.824(6)	P(1)–C(36)	1.807(5)
N(11)–C(12)	1.326(7)	N(11)–C(16)	1.339(6)
N(21)–C(22)	1.331(7)	N(21)–C(26)	1.343(6)
N(31)–C(32)	1.313(7)	N(31)–C(36)	1.338(6)
C(12)–C(13)	1.365(8)	C(13)–C(14)	1.345(9)
C(14)–C(15)	1.365(9)	C(15)–C(16)	1.367(7)
C(22)–C(23)	1.356(8)	C(23)–C(24)	1.348(9)
C(24)–C(25)	1.367(9)	C(25)–C(26)	1.363(7)
C(32)–C(33)	1.352(8)	C(33)–C(34)	1.355(8)
C(34)–C(35)	1.363(8)	C(35)–C(36)	1.381(7)
Cl–O(1)	1.346(6)	Cl–O(2)	1.371(6)
Cl–O(3)	1.371(6)	Cl–O(4)	1.391(5)
N(11)–Zn–N(21)	87.8(2)	N(11)–Zn–N(31)	88.5(2)
N(21)–Zn–N(31)	87.8(2)	C(16)–P(1)–C(26)	99.2(2)
C(16)–P(1)–C(36)	103.0(2)	C(26)–P(1)–C(36)	100.9(2)
Zn–N(11)–C(12)	120.5(4)	Zn–N(11)–C(16)	122.1(3)
Zn–N(21)–C(22)	120.5(4)	Zn–N(21)–C(26)	122.5(4)
Zn–N(31)–C(32)	121.5(4)	Zn–N(31)–C(36)	120.4(3)
C(12)–N(11)–C(16)	117.2(5)	C(22)–N(21)–C(26)	116.9(5)
C(32)–N(31)–C(36)	117.9(5)	N(11)–C(12)–C(13)	123.1(5)
C(12)–C(13)–C(14)	118.9(6)	C(13)–C(14)–C(15)	119.6(6)
C(14)–C(15)–C(16)	118.6(6)	P(1)–C(16)–N(11)	121.4(4)
P(1)–C(16)–C(15)	116.1(4)	N(11)–C(16)–C(15)	122.5(5)
N(21)–C(22)–C(23)	122.9(6)	C(22)–C(23)–C(24)	119.7(6)
C(23)–C(24)–C(25)	118.9(6)	C(24)–C(25)–C(26)	118.9(6)
P(1)–C(26)–N(21)	121.1(4)	P(1)–C(26)–C(25)	116.2(4)
N(21)–C(26)–C(25)	122.7(5)	N(31)–C(32)–C(33)	124.1(5)
C(32)–C(33)–C(34)	118.6(6)	C(33)–C(34)–C(35)	119.1(5)
C(34)–C(35)–C(36)	119.3(5)	P(1)–C(36)–N(31)	123.2(4)
P(1)–C(36)–C(35)	115.8(4)	N(31)–C(36)–C(35)	121.0(5)

**Fig. 3** Molecular structure and crystallographic numbering scheme for the cation in $[\text{Zn}\{\text{P}(\text{C}_5\text{H}_4\text{N})_3\}_2][\text{ClO}_4]_2 \cdot \text{H}_2\text{O}$

water molecules, 2.734(8) Å, occurs between a pair of O(1) atoms. There are two independent Zn–N bond distances with Zn–N(11) 2.123(5) Å ($\times 2$) being shorter than Zn–N(21) 2.141(3) Å ($\times 4$) and the maximum deviation from octahedral geometry is manifested in the N(11)–Zn–N(21) angle of 85.3(1)°.

$[\text{Zn}\{\text{P}(\text{C}_5\text{H}_4\text{N})_3\}_2][\text{ClO}_4]_2 \cdot \text{H}_2\text{O}$. The structure of the cation is shown in Fig. 3 and interatomic parameters are listed in Table 3. The closest non-H contact in the lattice occurs between the O(5) and C(33') atoms of 3.08(1) Å (symmetry operation: $\frac{1}{2} + x, \frac{1}{2} + y, 1 + z$). The cation is centrosymmetric with the

Zn–N(21) bond distance 2.145(4) Å being shorter than the others, *i.e.* Zn–N(11) 2.162(4) and Zn–N(31) 2.173(4) Å. The distortions from the ideal octahedral geometry are less in this complex, *i.e.* N(11)–Zn–N(21) is 87.8(2)°, owing to the longer P–C bonds.

Electronic spectra

The spectra of all complexes were recorded both as single crystals and KBr discs at room temperature (290 K) and ≈ 15 K. The room-temperature spectrum of $[\text{Ni}\{\text{CH}(\text{C}_5\text{H}_4\text{N})_3\}_2]^{2+}$ (Fig. 4) consists of a highly asymmetric peak centred at $\approx 13\,300\text{ cm}^{-1}$, with a shoulder at $\approx 14\,200\text{ cm}^{-1}$, and two peaks at 21 300 and 22 370 cm^{-1} , with a shoulder at $\approx 19\,000\text{ cm}^{-1}$. At 15 K the peaks tend to move slightly to higher energy. The lowest-energy pair of peaks are assigned to the ${}^3\text{T}_{2g}$ level of the parent octahedral complex, split by low-symmetry components of the ligand field. The asymmetry of the peak at 13 300 cm^{-1} may be due to the close proximity of the spin-forbidden ${}^1\text{E}$ transition, which is calculated to lie very close

to the ${}^3\text{E}$ level (Table 4). The shoulder at 19 000 cm^{-1} and the peak at $\approx 21\,300\text{ cm}^{-1}$ are assigned to the split components of the ${}^3\text{T}_{1g}(\text{F})$ level, with the remaining peaks being due to spin-forbidden transitions. The relatively high intensity of the peak at 22 370 cm^{-1} can be explained by its proximity to the neighbouring spin-allowed band. As with the $(\text{NC}_5\text{H}_4)_3\text{CH}$ complexes,² $[\text{Ni}\{\text{CH}(\text{C}_5\text{H}_4\text{N})_3\}_2]^{2+}$ belongs to the D_{3d} point group and thus the orbital triplet states are split into a singlet and a doublet. The selection rules indicate that polarized spectra will not differentiate the transitions, so that the assignment is based solely upon the AOM calculations. The band assignments are given in Table 4.

The spectrum of the $[\text{Ni}\{\text{P}(\text{C}_5\text{H}_4\text{N})_3\}_2]^{2+}$ complex was measured with both nitrate and perchlorate counter anions. The spectrum of the perchlorate salt was better resolved at low temperature and is shown in Fig. 5. The spectrum consists of an asymmetric peak centred at $\approx 13\,000\text{ cm}^{-1}$ with a shoulder at higher energy, and another asymmetric peak centred at $\approx 20\,000\text{ cm}^{-1}$ with a shoulder at $\approx 18\,500\text{ cm}^{-1}$ which is better resolved at low temperature. A weak peak can be seen at low temperature at about 20 600 cm^{-1} . The lowest-energy band is assigned to the ${}^3\text{T}_{2g}$ level of the parent octahedral complex, with the bands at 18 500 and $\approx 20\,000\text{ cm}^{-1}$ being due to components of the ${}^3\text{T}_{1g}(\text{F})$ level, the splittings being caused by the low symmetry of the ligand field. For this compound at room temperature, Holm and co-workers¹⁰ reported peaks at 11 500, 12 600 and 19 000 cm^{-1} and a number of far more intense ($\epsilon > 200\text{ dm}^3\text{ mol}^{-1}\text{ cm}^{-1}$) transitions at higher energy.

The single-crystal spectrum of the $[\text{Ni}\{\text{N}(\text{C}_5\text{H}_4\text{N})_3\}_2]^{2+}$ complex (Fig. 6) showed a band at $\approx 13\,300\text{ cm}^{-1}$, with shoulders at 13 000 and $\approx 14\,200\text{ cm}^{-1}$, and two peaks at 18 500 and 20 800 cm^{-1} , which are well resolved using polarized light. These may be compared with the peak energies¹¹ reported for the room-temperature reflectance spectra (10 700, 12 800, 19 050 and 26 800 cm^{-1}). The band assignments (Table 4) are similar to those of the other compounds studied in this work, in keeping with the proposed very similar structure, and thus it is assumed the spin-forbidden peak is at about 13 100

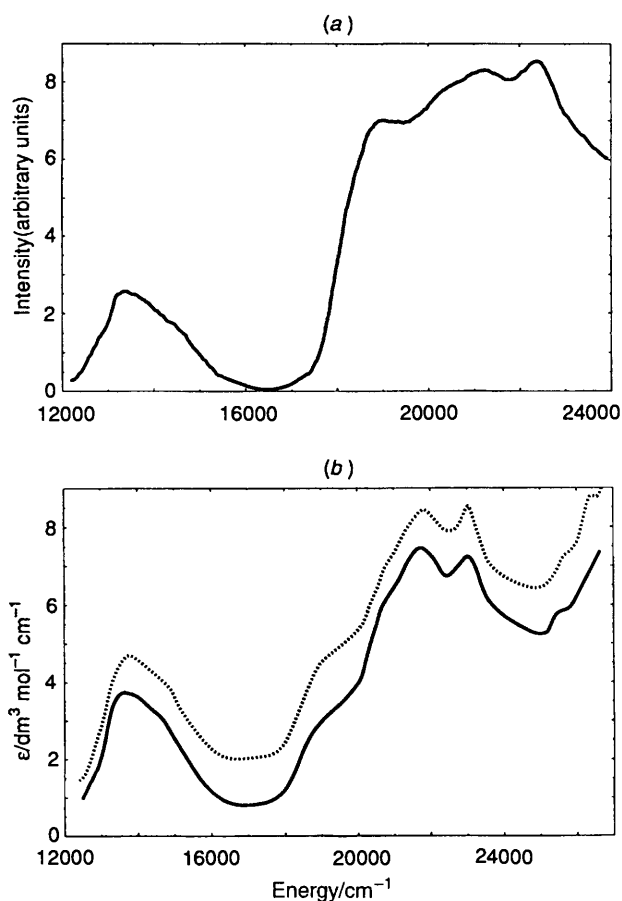


Fig. 4 Electronic spectrum of $[\text{Ni}\{\text{CH}(\text{C}_5\text{H}_4\text{N})_3\}_2][\text{NO}_3]_2$ recorded (a) as a KBr disc at ≈ 15 K and (b) as a single crystal at ≈ 15 K with the electric vector of the polarized light along each of the two extinction directions of a crystal face of unknown morphology

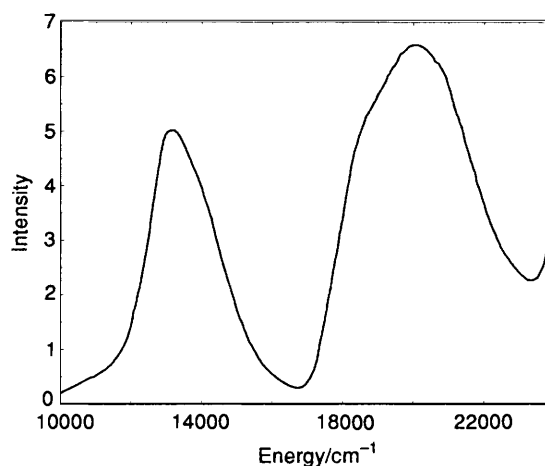


Fig. 5 Electronic spectrum of $[\text{Ni}\{\text{P}(\text{C}_5\text{H}_4\text{N})_3\}_2][\text{ClO}_4]_2$ measured as a KBr disc at ≈ 15 K

Table 4 Observed and calculated transition energies (cm^{-1})

Assignment	$[\text{Ni}\{\text{CH}(\text{C}_5\text{H}_4\text{N})_3\}_2]^{2+}$	$[\text{Ni}\{\text{P}(\text{C}_5\text{H}_4\text{N})_3\}_2]^{2+}$	$[\text{Ni}\{\text{N}(\text{C}_5\text{H}_4\text{N})_3\}_2]^{2+}$	Calculated
${}^3\text{A}_{1g} \rightarrow {}^3\text{A}_{2g} [{}^3\text{T}_{2g}(\text{F})]$	13 300	13 000	13 000	13 250
$\rightarrow {}^3\text{E}_g [{}^3\text{T}_{2g}(\text{F})]$	14 200	14 200?	14 200	14 300
$\rightarrow {}^1\text{E}_g$	$\approx 13\,500$	Not observed	Not observed	13 100
$\rightarrow {}^3\text{A}_{2g} [{}^3\text{T}_{1g}(\text{F})]$	18 500	18 500	18 500	18 800
$\rightarrow {}^3\text{E}_g [{}^3\text{T}_{1g}(\text{F})]$	21 300	20 500	20 800	21 500
$\rightarrow {}^1\text{A}_{1g}$	22 370	20 750	22 000	22 100

Parameters used: $e_\sigma = 5300$, $e_{\pi y} = 1040$ and $e_{\pi x} = 0\text{ cm}^{-1}$ in all cases; $B = 750$, $C = 3675\text{ cm}^{-1}$.

Table 5 Crystal data for the complexes

	[Ni{CH(C ₅ H ₄ N) ₃ } ₂]- [NO ₃] ₂	[Zn{CH(C ₅ H ₄ N) ₃ } ₂]- Br ₂ ·9H ₂ O	[Zn{P(C ₅ H ₄ N) ₃ } ₂]- [ClO ₄] ₂ ·H ₂ O
Formula	C ₃₂ H ₂₆ N ₈ NiO ₆	C ₃₂ H ₄₄ Br ₂ N ₆ O ₉ Zn	C ₃₀ H ₂₆ Cl ₂ N ₆ O ₉ P ₂ Zn
<i>M</i>	677.3	881.9	812.8
Crystal system	Trigonal	Monoclinic	Monoclinic
Space group	<i>R</i> $\bar{3}$	<i>C</i> 2/ <i>m</i>	<i>C</i> 2/ <i>c</i>
<i>a</i> /Å	11.655(3)	13.020(1)	24.041(1)
<i>b</i> /Å	—	13.221(1)	9.787(4)
<i>c</i> /Å	17.829(5)	11.053(2)	17.184(2)
β /°	90	104.22(1)	125.781(3)
<i>U</i> /Å ³	2097(1)	1844.3(3)	3280.2(9)
<i>Z</i>	3	2	4
<i>D_c</i> /g cm ⁻³	1.609	1.588	1.646
μ /cm ⁻¹	7.59	28.98	10.74
Maximum, minimum transmission factors	1.091, 0.833	1.032, 0.963	1.204–0.890
<i>F</i> (000)	1050	900	1656
No. of data measured	1229	2407	4242
Range <i>h k l</i>	–15 to 15, 0–15, 0–23	0–17, 0–17, –15 to 15	0–32, 0–13, –23 to 23
No. unique data	1114	2307	4143
<i>R</i> _{int} ^a	0.049	0.059	0.034
No. observed data [<i>I</i> ≥ 3.0σ(<i>I</i>)]	878	1621	2093
<i>R</i> ^b	0.043	0.041	0.049
<i>R</i> ^c	0.047	0.051	0.049
Goodness of fit ^d	1.18	2.89	1.10

^a $\sum_{i=1}^n \sum_{j=1}^m |<F_i^2> - F_{ij}^2| / \sum_{i=1}^n m <F_i^2>$ where *n* is the number of reflections measured more than once, *m* the number of times a given reflection has been measured and $\langle F_i^2 \rangle$ is the average value for *F*² for the unique reflection *i*. ^b $\sum_{i=1}^n (|F_{ol_i}| - |F_{cl_i}|) / \sum_{i=1}^n |F_{ol_i}|$. ^c $[\sum_{i=1}^n w_i (|F_{ol_i}| - |F_{cl_i}|)^2 / \sum_{i=1}^n w_i |F_{ol_i}|^2]^{\frac{1}{2}}$. ^d $[\sum_{i=1}^n (|F_{ol_i}| - |F_{cl_i}|) / \sigma_i] / (n - m)$ where *n* is the number of reflections used in refinement and *m* the number of variables.

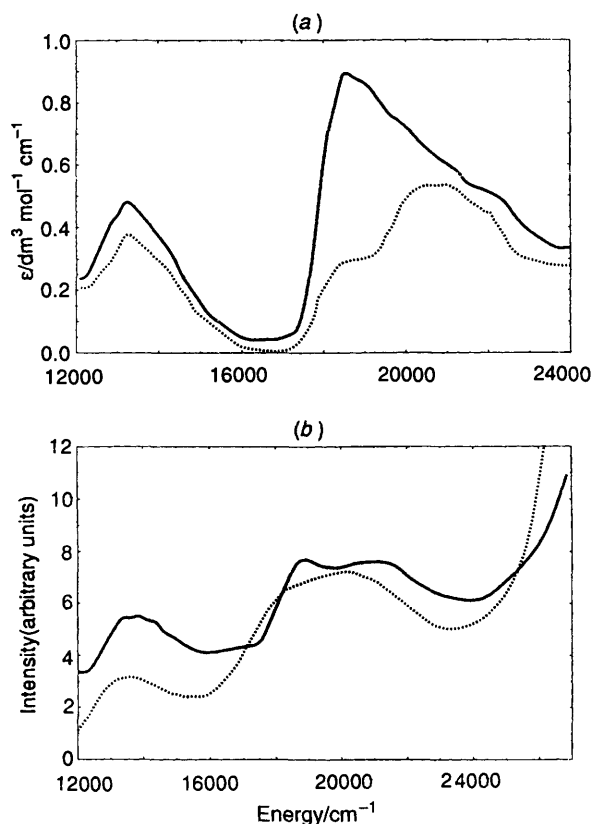


Fig. 6 Electronic spectra of [Ni{N(C₅H₄N)₃}₂][NO₃]₂ recorded (a) as a single crystal at ≈ 15 K with the electric vector of the polarized light along each of the two extinction directions of a crystal face of unknown morphology, and (b) as a KBr disc at room temperature (dashed line) and ≈ 15 K (solid line)

cm⁻¹, so that the observed band probably includes this, which may partly account for the asymmetrical nature of the first transition.

Metal–ligand bonding parameters

The relatively high energies of the 'd–d' transitions indicate the presence of a strong ligand field. This can be due either to π-acceptor character in the metal–ligand bonding, or the donor being positioned close to the metal ion. For other tripodal ligands like (pz)₃CH² and (pz)₂(NC₅H₄)CH¹ it has been shown that the second case is true.

To investigate the bonding characteristics of the compounds, the computer package CAMMAG, developed by Gerloch and co-workers,¹² was used to estimate the metal–ligand bonding parameters of the complexes within the framework of the AOM. The program calculates the transition energies of a complex, using as input σ- and π-bonding parameters of the ligand donor atoms and the molecular geometry indicated by the crystal structure. In the present case this involved the parameters *e_σ*, *e_{πx}* and *e_{πy}* for each pyridine group, where *e_{πx}* and *e_{πy}* describe the π bonding parallel and perpendicular to the plane of the amine ring, respectively. It should be noted that in mixed-ligand complexes it is impossible to determine all the bonding parameters independently, and it has usually been assumed that the *e_{πx}* parameter of ligands such as pyridine is zero.¹³ The present study provides an opportunity to test the validity of this assumption.

Without the crystal structures of the [Ni{P(C₅H₄N)₃}₂]²⁺ and [Ni{N(C₅H₄N)₃}₂]²⁺ complexes, unambiguous calculations of bonding parameters for these ligands are impossible. However, a comparison of the structures of similar complexes formed by P(C₅H₄N)₃ and N(C₅H₄N)₃ suggests³ that the effect on the co-ordination geometry (both bond lengths and angles) is minimal, so that the (NC₅H₄)₃CH structure could be used to gauge the bonding parameters. The spectra of all three compounds are similar, so it is not surprising that the same bonding parameters gave an adequate fit to the spectra. The results are shown in Table 4.

For each complex, the parameters reported¹ for the pyridine-type nitrogen of (pz)₂(NC₅H₄)CH, scaled as described previously to take into account the differences in bond lengths,¹ were used initially to calculate the excited-state energies of the complexes. The limited number of parameters to be determined

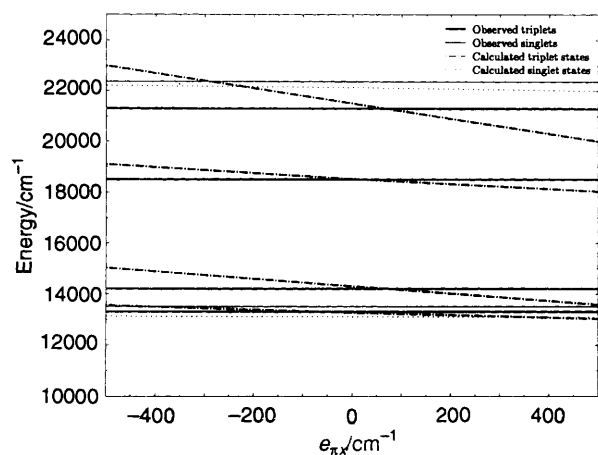


Fig. 7 Plot of the calculated transition energies as a function of $e_{\pi x}$

Table 6 Fractional atomic coordinates for the non-hydrogen atoms in $[\text{Ni}\{\text{CH}(\text{C}_5\text{H}_4\text{N})_3\}_2][\text{NO}_3]_2$

Atom	x	y	z
Ni ^a	1.0	0	1.0
O(1)	0.6668(4)	0.2279(3)	0.9775(2)
N(1) ^b	2/3	1/3	0.9709(4)
N(11)	0.9869(2)	0.1334(2)	0.9290(1)
C(1) ^b	1.0	0	0.8297(3)
C(12)	0.9726(3)	0.2345(3)	0.9528(2)
C(13)	0.9604(4)	0.3189(3)	0.9062(2)
C(14)	0.9645(3)	0.3024(3)	0.8301(2)
C(15)	0.9811(3)	0.2008(3)	0.8045(2)
C(16)	0.9901(3)	0.1172(3)	0.8551(2)

^a Atom has site occupancy factor 1/6. ^b Atom has site occupancy factor 1/3.

Table 7 Fractional atomic coordinates for the non-hydrogen atoms in $[\text{Zn}\{\text{CH}(\text{C}_5\text{H}_4\text{N})_3\}_2]\text{Br}_2 \cdot 9\text{H}_2\text{O}$

Atom	x	y	z
Br ^a	0.610 45(5)	0	0.300 15(7)
Zn ^b	0	0	0
O(1)	0.653 1(3)	0.234 5(3)	0.419 9(4)
O(2) ^a	1.0	0.155 6(4)	0.5
O(3) ^a	0.885 5(4)	0	0.357 2(4)
O(4) ^b	0.5	0.072 6(19)	1.0
N(11) ^a	0.135 7(4)	0	0.152 7(4)
N(21) ^a	0.083 9(2)	0.110 6(3)	-0.079 9(3)
C(1) ^a	0.235 8(4)	0	-0.006 4(5)
C(12) ^a	0.130 8(5)	0	0.270 6(6)
C(13) ^a	0.218 5(6)	0	0.368 5(6)
C(14) ^a	0.315 6(5)	0	0.341 9(6)
C(15) ^a	0.321 9(5)	0	0.221 2(6)
C(16) ^a	0.231 2(4)	0	0.128 3(5)
C(22)	0.038 3(3)	0.191 1(3)	-0.140 9(4)
C(23)	0.090 1(4)	0.257 6(4)	-0.198 7(4)
C(24)	0.194 8(4)	0.239 7(4)	-0.192 6(4)
C(25)	0.243 1(3)	0.157 6(3)	-0.128 3(4)
C(26)	0.185 7(3)	0.094 0(3)	-0.074 0(4)

^a Atom has site occupancy factor 0.5. ^b Atom has site occupancy factor 0.25.

meant that there was no need to restrain $e_{\pi x}$ to 0. Initial calculations with $e_{\pi x} = 0$ and the scaled parameters provided an excellent fit, with most calculated transition energies being within 300 cm^{-1} of those observed experimentally. The Racah parameters were reduced to $\approx 75\%$ of their free-ion values,¹⁴ which is in good agreement with the results for the corresponding $(\text{pz})_3\text{CH}$ complex.² The sensitivity of the calculated transition energies to the π -bonding was investigated by changing $e_{\pi x}$ while keeping the other parameters unaltered and the effect is shown in Fig. 7. While the fit to the splitting of

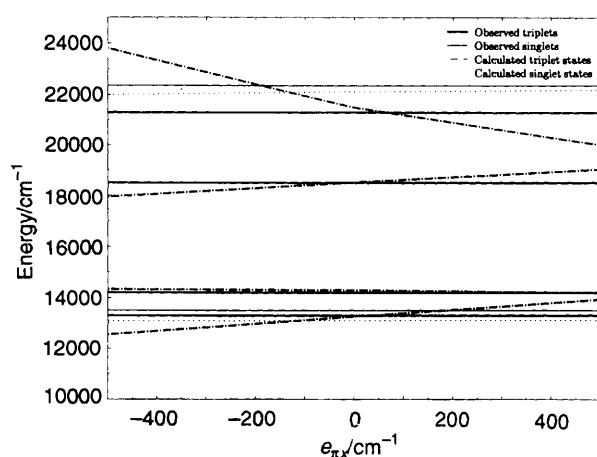


Fig. 8 Plot of the calculated transition energies as a function of $e_{\pi x}$ (with Δ constant)

Table 8 Fractional atomic coordinates for the non-hydrogen atoms of $[\text{Zn}\{\text{P}(\text{C}_5\text{H}_4\text{N})_3\}_2][\text{ClO}_4]_2 \cdot \text{H}_2\text{O}$

Atom	x	y	z
Zn *	0	0	0
Cl	0.3594(8)	0.0125(2)	0.0275(1)
P(1)	0.1750(7)	0.0353(1)	0.1631(1)
O(1)	0.4208(3)	0.0741(8)	0.0716(5)
O(2)	0.3489(4)	-0.0834(7)	-0.0380(5)
O(3)	0.3094(4)	0.1110(9)	-0.0159(5)
O(4)	0.3552(4)	-0.0445(6)	0.0980(4)
O(5) *	0.5	0.1605(12)	0.75
N(11)	0.0551(2)	0.1837(4)	0.0763(3)
N(21)	0.0648(2)	-0.1088(4)	0.1326(3)
N(31)	0.0767(2)	-0.0373(4)	-0.0266(3)
C(12)	0.0214(3)	0.2979(6)	0.0652(4)
C(13)	0.0531(4)	0.4142(6)	0.1162(5)
C(14)	0.1216(4)	0.4141(7)	0.1808(6)
C(15)	0.1579(3)	0.2981(6)	0.1949(5)
C(16)	0.1233(3)	0.1855(5)	0.1406(4)
C(22)	0.0383(3)	-0.1992(6)	0.1603(4)
C(23)	0.0763(4)	-0.2650(6)	0.2458(5)
C(24)	0.1440(4)	-0.2391(7)	0.3069(5)
C(25)	0.1731(3)	-0.1481(6)	0.2802(4)
C(26)	0.1326(3)	-0.0860(5)	0.1930(4)
C(32)	0.0597(3)	-0.0827(6)	-0.1097(4)
C(33)	0.1053(3)	-0.1138(7)	-0.1288(4)
C(34)	0.1730(3)	-0.0947(7)	-0.0590(5)
C(35)	0.1927(3)	-0.0476(6)	0.0284(4)
C(36)	0.1434(3)	-0.0210(5)	0.0437(4)

* Atom has site occupancy factor 0.5.

the ${}^3\text{T}_1(\text{F})$ level is best with an $e_{\pi x}$ value of about $+200 \text{ cm}^{-1}$, the splitting of the ${}^3\text{T}_2(\text{F})$ level is better with $e_{\pi x} = -200 \text{ cm}^{-1}$. By keeping Δ the same (by decreasing $e_{\pi y}$ as $e_{\pi x}$ is increased) the best fit is clearly found with $e_{\pi x}$ close to zero (see Fig. 8). Variation of the other parameters was also tested and no substantially improved fit was obtained. The results of the best fit are shown in Table 4. The parameters, $e_{\sigma} = 5300$ and $e_{\pi y} = 1040 \text{ cm}^{-1}$, found for all three complexes, compare well with those for the slightly longer nickel-pyridine interaction in $[\text{Ni}\{\text{CH}(\text{C}_5\text{H}_4)(\text{pz})_2\}_2]^{2+}$ where $e_{\sigma} = 5175$ and $e_{\pi y} = 1020 \text{ cm}^{-1}$.¹ The fact that different parameters were not required for the nitrogen nor phosphorus bridgehead ligands indicates that conjugation between the rings, possible in these ligands but impossible in the carbon bridgehead ligand, is not required to explain their electronic properties.

Conclusion

The molecular geometries of the complexes are very similar, and to those of other complexes formed by similar tripodal ligands.

The large ligand-field splitting observed for each complex is due to the relatively strong σ -donor and moderate π -donor capacity of the ligands, this probably being caused by the relatively short M–N bonds in the compounds. The bonding parameters of the three ligands are indistinguishable, suggesting that the nature of the bridgehead atom has little effect on the metal–ligand interaction. In particular, the π -bonding parameters provide no evidence for conjugation of the π systems in any of the ligands. In agreement with McWhinnie *et al.*¹¹ we find that ‘conjugation within polypyridyl ligands is not a prerequisite for high values of Δ ’. In agreement with simple theory, no notable degree of in-plane π bonding was detected.

Acknowledgements

The financial support of the Australian Research Council is acknowledged and Dr. M. Gerloch, Cambridge University Chemical Laboratory, is thanked for making available the computer package CAMMAG. The assistance of Mr. P. A. Anderson and Mr. R. J. A. Janssen in the initial stages of the syntheses is acknowledged.

References

- 1 T. Astley, A. J. Canty, M. A. Hitchman, G. L. Rowbottom, B. W. Skelton and A. H. White, *J. Chem. Soc., Dalton Trans.*, 1991, 1981.
- 2 T. Astley, J. M. Gulbis, M. A. Hitchman and E. R. T. Tienkink, *J. Chem. Soc., Dalton Trans.*, 1993, 509.
- 3 F. R. Keene, M. R. Snow, P. J. Stephenson and E. R. T. Tienkink, *Inorg. Chem.*, 1988, **27**, 2040.
- 4 M. A. Hitchman, *Transition Met. Chem.*, 1985, **9**, 1.
- 5 N. Walker and D. Stuart, *Acta Crystallogr., Sect. A*, 1983, **39**, 158.
- 6 TEXSAN, Structure Analysis Package, Molecular Structure Corporation, Houston, TX, 1992.
- 7 C. K. Johnson, ORTEP II, Report ORNL-5136, Oak Ridge National Laboratory, Oak Ridge, TN, 1976.
- 8 T. Astley, P. J. Ellis, H. C. Freeman, M. A. Hitchman, F. R. Keene and E. R. T. Tienkink, *J. Chem. Soc., Dalton Trans.*, 1995, 595.
- 9 G. J. Long and P. J. Clarke, *Inorg. Chem.*, 1978, **17**, 1394; D. J. Hamm, J. Bordner and A. F. Schreiner, *Inorg. Chim. Acta*, 1973, **7**, 637.
- 10 E. Larsen, G. N. La Mar, B. E. Wagner, J. E. Parks and R. H. Holm, *Inorg. Chem.*, 1972, **11**, 2652.
- 11 W. R. McWhinnie, G. C. Kulasingham and J. C. Draper, *J. Chem. Soc. A*, 1996, 1199.
- 12 D. A. Cruse, J. E. Davies, M. Gerloch, J. Harding, D. Mackey and R. F. McMeeking, CAMMAG, a FORTRAN computing package, University of Cambridge, 1979.
- 13 B. J. Kennedy, K. S. Murray, M. A. Hitchman and G. L. Rowbottom, *J. Chem. Soc., Dalton Trans.*, 1987, 825.
- 14 A. B. P. Lever, *Inorganic Electronic Spectroscopy*, 2nd edn., Elsevier, Amsterdam, 1984, p. 115.

Received 11th September 1995; Paper 5/060101